NSRRC-J05287(2016)

Materials Views
www.MaterialsViews.com

ADVANCED MATERIALS INTERFACES
www.advmatinterfaces.de

COMMUNICATION

Surface Energy-Mediated Self-Patterning for High Performance Spray-Deposited Organic Field Effect Transistors

*Han-Wen Hsu, Wei-Chieh Chang, Shih-Huang Tung, and Cheng-Liang Liu**

Organic field effect transistors (OFETs) have attracted extensive research interest due to their potential applications in large area, mechanically flexible, light weight, and low-cost devices/circuits.[1–6] Solution processing of organic semiconductors offers versatility with respect to fine-tuning film qualities and morphologies while also being promising for dramatically reducing the manufacturing cost compared to current vacuum vapor phase deposition.[7–9] Among these effective techniques, spray-coating is considered to be one of most promising methods to deposit thin layers of organic semiconductors for large area devices with the advantages of controlled thickness and avoiding wasting materials during processing.[10–15] There are several continuous steps in the spray-coating process including atomization of solution particles, droplet flight onto the substrate driven by carrier gas, spreading, drying, and film formation. Most importantly, the thin film condition can be manipulated through the processing parameters without using expensive equipment.

Since the conventional lithography encounters the problems such as masking, high-vacuum deposition and etching, printing and related solution processing have gained considerable attention toward organic electronics in recent years.[16–24] Printing is a convenient processing technique for simple and high throughput manufacturing on the electronic devices, which requires a scalable and compatible patterning methodology for soluble components to deposit in a controlled manner. Surface energy-mediated self-organization of thin film is a nonlithographic method toward assembling of organic semiconductors into regular patterns,[25–36] which can be achieved by varying the functional groups of the self-assembly monolayers (SAM) used to modify the dielectric surface. The difference in surface energy provides a driving force for solution-processed organic semiconductors to preferentially wet within the desired regions where the growth of the organic semiconductors is strongly influenced by the surface characteristics.[37–39] The resulting macroscale morphologies and microscale molecular orientation of the assembly organic semiconductor patterns can simultaneously determine the charge carrier mobility of the OFETs.

To the best of our knowledge, the spray-deposition of patterned active semiconducting layer for large area OFETs and its detailed film morphologies, molecular packing, and electrical properties have not been reported yet. Here, we develop a new strategy to combine the bottom-up surface energy-mediated self-patterning technique and top-down spray-coating process to fabricate patterned OFETs. The focus of this study was to investigate the self-patterning behaviors of the solution-processable organic semiconductors, morphology of the fabricated films, and the resulted electrical properties of the spray-deposited OFETs. The studied materials include 6,13-bis(triisopropylsilylethynyl)pentacene (TIPS-PEN) and poly(selenophene-alt-3,6-dithophene-2-yl-2,5-bis-(2-hexyldecyl)-2,5-dihydro-pyrrolo[3,4-c]pyrrole-1,4-dione) (PSeDPP). The obtained patterned OFETs of TIPS-PEN and PSeDPP exhibited relatively high-charge mobilities of more than 1 and 5 $cm^2 V^{-1} s^{-1}$, respectively, which could be also extended to a large area of the well-ordered patterning of OFETs array. The developed approach can contribute to the mass production on the solution-processed and patternable OFETs with controllable electrical characteristics without a complicated lithography process.

A schematic depiction on the spray deposition of the organic semiconductors, TIPS-PEN and PSeDPP, onto the surface pattern of the SiO_2 layers is created using the combination of UV/ozone treatment and silane modification, as shown in **Figure 1**. The patterned stripes for depositing organic semiconductors were fabricated based on surface wettable/dewettable regions involving the substrate surface modification with different functional groups of SAM. First, the sample was immersed in a diluted octadecyltrichlorosilane (ODTS) solution (Figure 1c) to allow the ODTS passivation to self-assemble on the dielectric surface, as the solution-repellent region (Figure 1d). Subsequently, the ODTS SAM was irradiated with UV/ozone for 15 min through a shadow mask to create stripe areas (Figure 1e) on which the hydrophobic alkyl chains of ODTS are removed to form hydrophilic surface (Figure 1g).[40,41] These regions were then treated with other silanes (for example, shorter alkyl or phenyl tail groups) to form SAM that has higher surface energy and are more favorable for depositing π-conjugated organic semiconductor (Figure 1h). After that, the prepared organic semiconductor solution was spray-deposited onto the patterned substrate (Figure 1i). Due to the higher surface energy of the stripe areas, the organic semiconductor solution tends to dewet from the hydrophobic ODTS area/wet on the stripe areas. The resulting TIPS-PEN crystalline grains selectively deposited on

H.-W. Hsu, W.-C. Chang, Prof. C.-L. Liu
Department of Chemical and Materials Engineering
National Central University
Taoyuan 32001, Taiwan
E-mail: clliu@ncu.edu.tw
Prof. S.-H. Tung
Institute of Polymer Science and Engineering
National Taiwan University
Taipei 10617, Taiwan

DOI: 10.1002/admi.201500714

 © 2016 WILEY-VCH Verlag GmbH & Co. KGaA, Weinheim

ADVANCED MATERIALS INTERFACES
www.advmatinterfaces.de

Materials Views
www.MaterialsViews.com

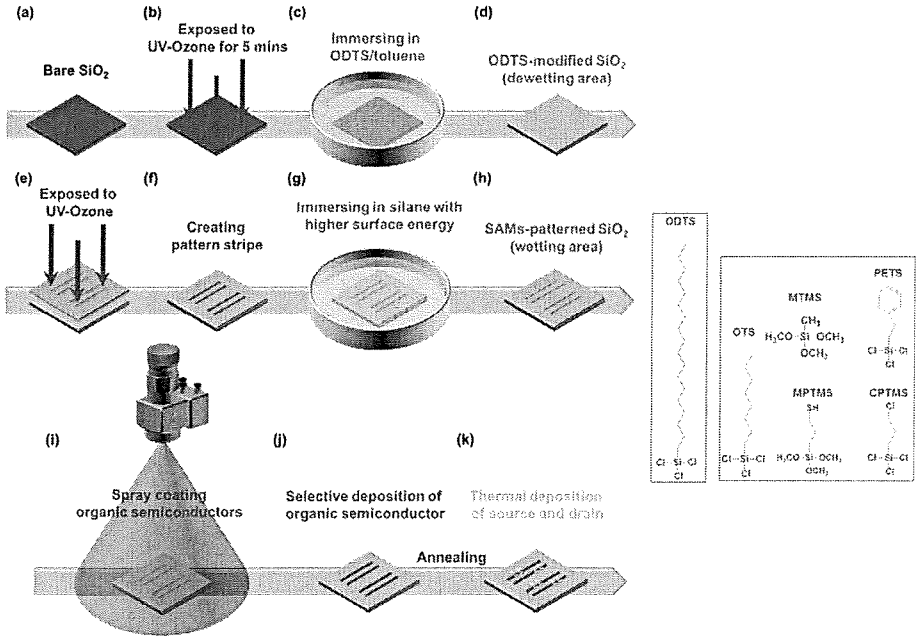

Figure 1. Schematic illustration of surface energy-mediated self-patterning for the spray-deposited OFETs and chemical structures of silanes used in this work.

the micropatterned substrates with the SAM regions of (2-phenylethyl)trichlorosilane (PETS), octyltrichlorosilane (OTS), methyltrimethoxysilane (MTMS), (3-mercaptopropyl)trimethoxysilane (MPTMS), and 3-chloropropyltrichlorosilane (CPTS) are shown in **Figure 2**a and Figure S1 (Supporting Information), respectively. The stripes with the organic semiconductor crystal grains were then applied for the channels of the OFETs.

Figure S2 (Supporting Information) presents the results of the contact angle measurement and corresponding surface energy of various SAM-treated SiO_2 surfaces. An ODTS-modified surface becomes hydrophobic (water contact angle ≈109.3°) and hardly wetted, which is indicative of a low-surface energy (18.2 mJ m^{-2}). The water contact angle of other silane SAM-treated surfaces decreases to the range between 63.3° and 106.7°, showing a better wettability than ODTS and implying a higher surface energy (24.7–46.0 mJ m^{-2}). Patterned thin film of the semiconducting TIPS-PEN by the use of solution in 1,2-dichlorobenzene (DCB) was first examined. The capillary force caused by the surface energy differences on the top of the substrate directs the TIPS-PEN solution toward the patterned area in order to reduce the surface energy. In addition to the surface energy, solvent evaporation during the drying process may affect the solution flow property and thus also plays an important role in the distribution and the crystal growth of TIPS-PEN. The amount of remaining solvent on the substrate during dewetting process is dependent on how far the substrate away from the nozzle. Thus, the relationship between wetting/dewetting phenomena and the patterned substrate that is placed in different heights of the patterned substrate away from nozzle tip needs to be established. Optical microscopy images of TIPS-PEN deposited on the PETS-patterned substrates with 9–13 cm working distances from the nozzle to the substrates are shown in Figure S3a–e (Supporting Information). When the nozzle is placed far from the substrate (Figure S3a–c, Supporting Information), because the TIPS-PEN solution is dried before reaching the patterned area, isolated TIPS-PEN crystals sporadically form on the whole substrate, without formation of continuous channels. When the nozzle is too close from the substrate, the drying process is slowed down and a great amount of TIPS-PEN solution concentrate on the patterned area, which leads to a thick film with randomly oriented TIPS-PEN crystals (Figure S3e, Supporting Information). To obtain a better selective patterning film, the nozzle is placed in an intermediate position, i.e., 10 cm (Figure S3d, Supporting Information), with which the combination of the drying process and the capillary force drives the sprayed TIPS-PEN solution onto the confined stripe areas where TIPS-PEN can crystallize in an ordered manner.

The electrical characteristics of the fabricated OFETs devices were measured through bottom-gate top-contact device configuration. The stripe pattern with ~100 μm width was selectively deposited by TIPS-PEN under optimized spray conditions (Figure 2a–c exhibits the typical output and transfer characteristics of the TIPS-PEN OFETs that is patterned with PETS SAM, respectively. All the electrical characteristics of corresponding TIPS-PEN OFETs with patterned channels based on other SAM modifications are shown in Figures S4 and S5 (Supporting Information). For comparisons, the morphologies of the unpatterned TIPS-PEN film by spray coating on varying SAM over the whole surface and the corresponding electrical properties are displayed in Figures S6 and S7 (Supporting Information), respectively. The saturated field effect mobility (μ) was calculated using the conventional field effect transistor model shown in Equation (1)

© 2016 WILEY-VCH Verlag GmbH & Co. KGaA, Weinheim

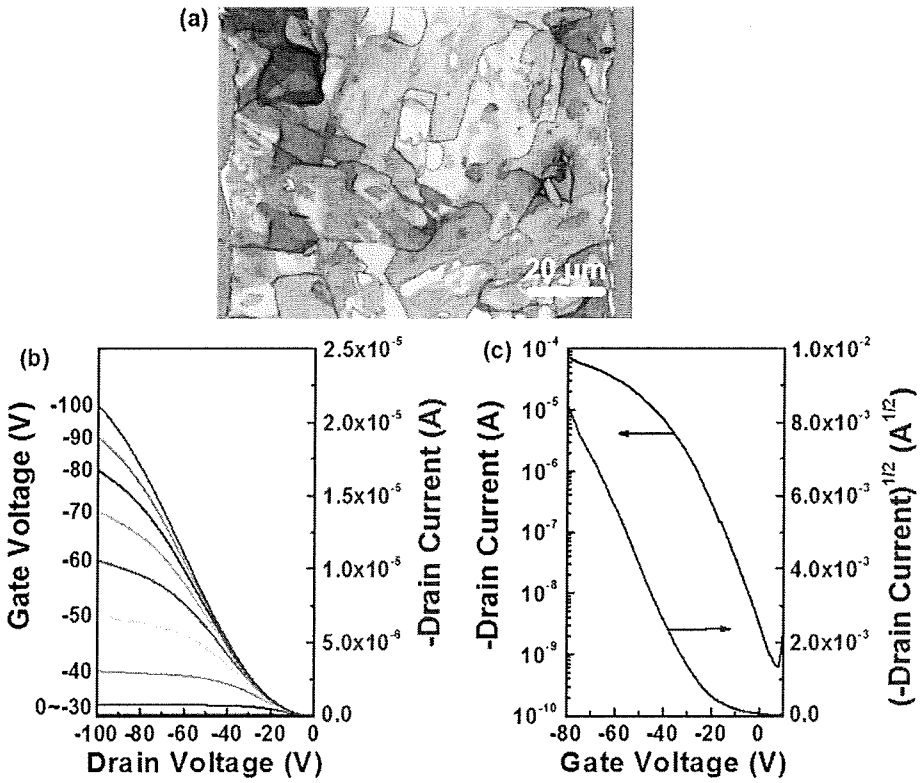

Figure 2. a) Optical image of the spray-coated TIPS-PEN film in a patterned region based on PETS SAM modification. b) Output and c) transfer curves of PETS SAM patterned TIPS-PEN OFETs.

$$I_d = \frac{WC}{2L}\mu(V_g - V_{th})^2 \quad (1)$$

where I_d is the drain current, C is the dielectric capacitance per unit area, V_g is the gate voltage, and V_{th} is the threshold voltage. The channels of dimension width (W)/length (L) = 1000 μm/25 μm were provided. As the OFETs consist of single stripe pattern, the effective channel width is determined by the width of each stripe (~100 μm). The electrical properties of the fabricated OFETs using a spray-deposited active layer on various SAM-modified substrates are listed in **Table 1**. The TIPS-PEN films without patterning result in lower hole mobilities of 0.01–0.06 $cm^2\ V^{-1}\ s^{-1}$, depending on the type of SAM modification. In contrast, the hole mobilities of the OFETs based on OTS, MTMS, MPTMS, and CPTS-SAM patterned films are higher, between 0.03 and 0.18 $cm^2\ V^{-1}\ s^{-1}$. In particular, the OFETs based on PETS-SAM patterned film present a mobility as high as 1.18 $cm^2\ V^{-1}\ s^{-1}$ and an ON/OFF ratio of five orders of magnitude. The results demonstrate that the field effect mobility can be dramatically improved through selective deposition of TIPS-PEN layer on 100 μm width patterned SAM strips with higher surface energy. Note that 100 μm is nearly the narrowest stripe width the simple shadow mask method can reach without photolithography. Previous report from Bao and co-workers has shown that the mobility of the solution-shearing TIPS-PEN film for patterned OFETs increases as the stripe width becomes smaller since greater lateral confinement induces better lateral alignment during crystal growth.[35] Although the pattern width is not fully optimized here, we believe that the alignment of TIPS-PEN molecules and the charge transport properties may be further improved if the linewidth can be further reduced by the photolithography method.

It is known that the electrical properties of organic semiconductors are highly dependent on the spatial arrangement of molecules. We thus used grazing incidence X-ray diffraction (GIXRD) to probe the orientation of molecular packing along the patterned channels. **Figure 3** shows the GIXRD images of the unpatterned and patterned TIPS-PEN films on PETS-SAM. For the unpatterned TIPS-PEN film, both (10l) and (01l) Bragg peaks are clearly observed (Figure 3a),[42–44] indicating the a- and b-axis of the TIPS-PEN crystal randomly rotate in the film plane. The c-axis is in the out of plane direction. Figure 3b shows the diffraction image of the patterned film with the incident beam parallel to the direction of the stripe. Different from the equally bright spots in Figure 3a, the intensity of the (10l) Bragg peaks are apparently stronger than that of the (01l) peaks. Such a diffraction pattern implies the a-axis is dominantly perpendicular to the stripe direction. In other words, the b-axis prefers to align along the stripe direction. This preferential orientation can be further confirmed by the diffraction image with the incident beam perpendicular to the stripes shown in Figure 3c where the (01l) peaks become more pronounced than the (10l) peaks. In a TIPS-PEN crystal, it has been shown that the charge transport is more efficient along the b-axis.[43] The orientation of the TIPS-PEN crystal induced by the dewetting force can thus exactly promote the charge mobility along

 © 2016 WILEY-VCH Verlag GmbH & Co. KGaA, Weinheim

Table 1. Electrical properties of unpatterned and patterned OFETs through spray deposition.

Organic semiconductors	SAM	Film condition	Mobility [$cm^2 V^{-1} s^{-1}$]	ON/OFF ratio	Threshold voltage [V]
TIPS-PEN	OTS	Unpatterned	0.01	6.3×10^4	−8.8
		Patterned	0.03	7.1×10^3	−16.6
	MTMS	Unpatterned	0.05	6.8×10^3	−21.9
		Patterned	0.13	2.8×10^3	−20.5
	PETS	Unpatterned	0.06	6.5×10^3	−10.9
		Patterned	1.18	1.4×10^5	−24.4
	MPTMS	Unpatterned	0.04	2.8×10^3	−20.5
		Patterned	0.18	7.8×10^5	−18.1
	CPTS	Unpatterned	0.01	7.6×10^2	−8.1
		Patterned	0.06	5.4×10^5	−20.6
PSeDPP	OTS	Unpatterned	0.29[a]/0.01[b]	$4.4 \times 10^3/4.2 \times 10^2$	−27.6/93.1
	OTS	Patterned	5.03[a]/0.43[b]	$2.3 \times 10^2/4.8 \times 10^2$	−32.0/91.5
	PETS	Unpatterned	0.08[a]/0.0001[b]	$4.4 \times 10^3/8.6 \times 10^3$	−26.9/86.1
	PETS	Patterned	3.45[a]/0.04[b]	$2.6 \times 10^4/4.3 \times 10^3$	−32.1/92.6

[a]Hole mobility; [b]Electron mobility.

the stripes. The proposed molecular packing within the TIPS-PEN films on unpatterned and patterned surface is depicted in Figure S8 (Supporting Information).

The functional groups on the SAM also affect the electrical properties. Well-wetting in the patterned stripes is introduced by the SAM with a higher surface energy relative to the outer ODTS-modified area. It increases the contact area between the TIPS-PEN and patterned substrate and favors continuous TIPS-PEN crystal attachment on all these five SAM-modified patterns, as shown in Figure 2a and Figure S1 (Supporting Information). However, the charge modulation of TIPS-PEN channel on the SAM interlayer is influenced by the interactions between the TIPS-PEN molecule and the specific functional groups of the SAM, reflecting the changes in the mobility of the electrical OFETs characteristics (Table 1). The SAM with highly polar functionalities, such as thiol (MPTMS) and chlorol (CPTS) groups, brings about limited improvement of the electrical characteristics of the pattered OFETs, probably due to the trapped interface charges.[21] Compared with the SAM molecules with a short alkyl chain (MTMS), the phenyl moieties-modified surface (PETS SAM) that can form π-interaction with TIPS-PEN molecules lead to a greatly improved molecular packing and charge transfer mobility. The value of saturated I_d for the patterned OFETs using the PETS SAM is one order of magnitude higher than those of the patterned OFETs with other silane modifications. It suggests that externally applied gate bias leads to a pronounced current contrast by selectively modifying the dielectric functional groups.

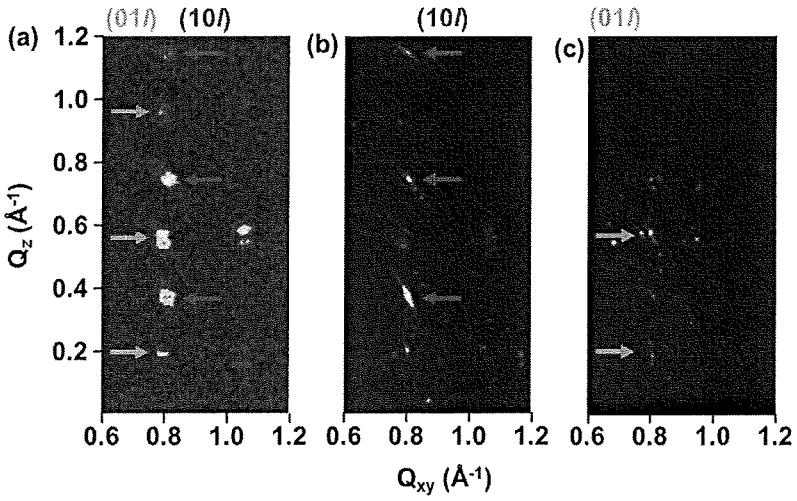

Figure 3. GIXRD images of spray-coated a) unpatterned film, b,c) patterned film, highlighting the (01*l*) and (10*l*) peak. The incident X-ray is parallel with respect to the patterned stripe direction in (b) and perpendicular in (c).

The applicability of the proposed method to polymeric semiconductors was explored by using an ambipolar conjugated polymer PSeDPP. The droplet and resulting polymer domain sizes can be finely tuned by controlling atomization process. The optical image of spray-coated PSeDPP on the patterned substrate modified with OTS is shown in Figure 4a. PSeDPP also wets the patterned region and forms overlapped ring-like structure with high roughness, indicating that originally separated droplets merge together in the wetting region and the surface coverage on this region is significantly increased. Figure 4b,c shows the representative transfer and output characteristics of optimized PSeDPP-based patterned OFETs on OTS SAM and the performances of the OFETs are summarized in Table 1. V-shaped ambipolar characteristics are clearly observed in the hole-enhancement (at drain voltage (V_d) = −100 V) and electron-enhancement

© 2016 WILEY-VCH Verlag GmbH & Co. KGaA, Weinheim

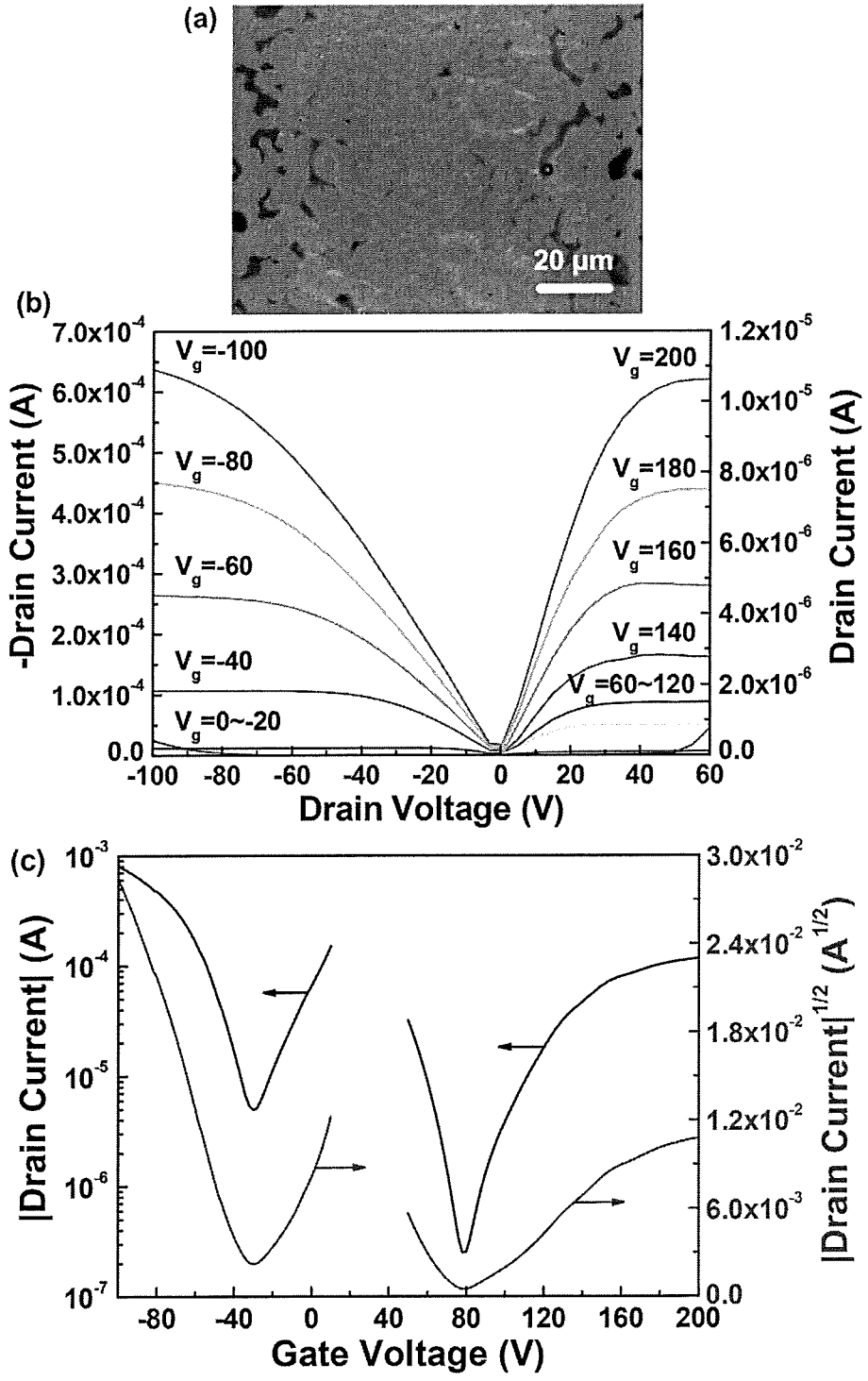

Figure 4. a) Optical image of the spray-coated PSeDPP film in a patterned region based on OTS SAM modification. b) Output and c) transfer curves of OTS SAM patterned PSeDPP OFETs.

(at V_d = 60 V) mode. The hole and electron mobilities of patterned OFETs measured from the OTS SAM patterned surface are up to 5.03 and 0.43 $cm^2\ V^{-1}\ s^{-1}$, respectively, which are much higher than the mobilities of the previously reported spin-coated[45] or spray-coated OFETs without patterning condition (Figure S9, Supporting Information). Similar significant

 © 2016 WILEY-VCH Verlag GmbH & Co. KGaA, Weinheim

enhancement in device performance is also observed in the PETS SAM patterned OFETs (Figure S10, Supporting Information) relative to unpatterned one (Figure S11, Supporting Information). We believe that the pronounced improvement in molecular ordering upon the semiconductors growth over the wettable surface facilitates charge hopping between the polymers chains. It should be again pointed out that the efficient charge transport between organic semiconductor molecules processed from spray deposition onto patterned device cells leads to the dramatic increase in I_d and results in higher carrier mobilities extracted from saturated region.

Our direct patterning strategies combined with spray deposition are practical for the precise production of high density and desired pattern of OFETs over large area. Patterned OFETs array composed of 8 × 8 device layout was fabricated on 4 inch Si wafer, as shown in **Figure 5**a. The PSeDPP solution was fed into the spray head and atomized by compressed air. The nozzle is positioned above the stationary stage onto which the patterned 4 in. Si substrate is tapped and its movement is controlled by a stepper motor programmably driven in X–Y direction. To ensure uniform coating and repeatability, the spraying movement with a sprayer traverse of 14 cm is vertical to the direction of patterned stripe under a drive speed of 5 cm s^{-1} until a total of repeated 20 times were deposited to spray onto whole surface. Figure 5b,c shows the optical microscope images of the OFETs array on patterned PETS SAM in device cell and the formation of stripe-shaped PSeDPP film can be seen. The transfer characteristics of all the 64 device cells are plotted in Figure 5d. The measured mobility and threshold voltage value in each cell are expressed by varying color in the 2D mapping plot as shown in Figure 5e,f. Note that the PSeDPP aggregated spots outside the patterned area, which do not reveal any electrical performance, as shown in Figure S12 (Supporting Information). It should be emphasized that all the OFETs operate well without failures and device cells reveal an average mobility of 0.63 ± 0.33 cm^2 V^{-1} s^{-1} with a maximum value of 1.58 cm^2 V^{-1} s^{-1}. The average threshold voltage is −5.9 ± 4.9 V and the ON/OFF current ratio lies between 10^3 and 10^4. The variation in electrical performance within the OFETs array may be caused by the imperfect SAM modification of pattern or the difference in semiconductor film thickness over the whole Si wafer substrate, which causes a fluctuation in the crystallinity or chain orientation of the semiconductor layer. Thus, the direct spray deposition of polymeric semiconductors by precise positioning can ensure a high quality of patterned device array although it has a slight reduction in mobility as compared to the previous single device cell with a fixed spraying. The high yield of the operational OFETs array clearly demonstrates the great potential for optimizing the processing conditions to achieve directly patterned assembling of the organic semiconductors on selective regions toward large area OFETs applications.

The method developed in this work is advantageous in the following aspects. Device fabrication by spray deposition on the surfaces with patterned wettability can offer the opportunity for the large scale and high throughput device fabrication. The development for practical solution-assembly of organic

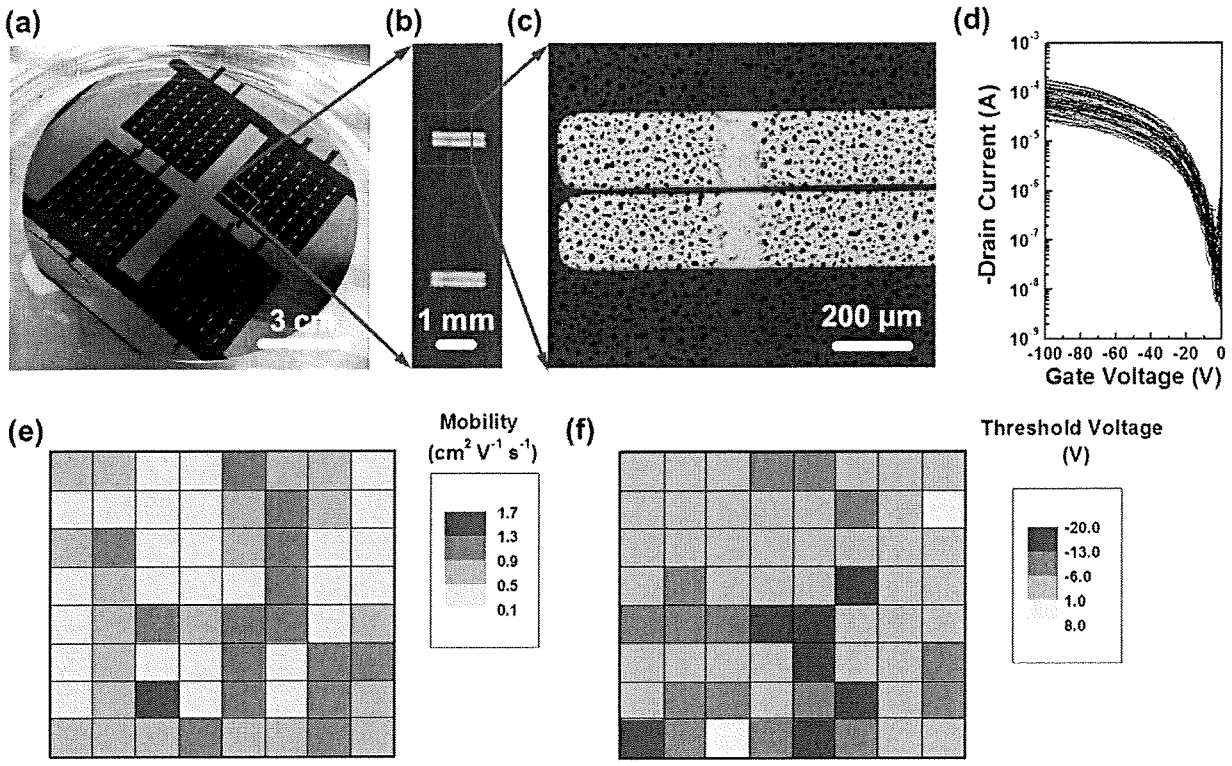

Figure 5. a) Photograph of patterned PSeDPP OFETs array on 4 inch wafers. b,c) Magnified view of each patterned OFETs cells. d) Transfer curves and mapping plot of the extracted e) hole mobility and f) threshold voltage for all 64 patterned OFETs device cells.

© 2016 WILEY-VCH Verlag GmbH & Co. KGaA, Weinheim

semiconductors directly on the required device location to form definite shape of the patterned film and the utilization of the inherent interface condition of gate dielectric can be readily adapted to a full realization of low-cost process. In addition, the entire spray deposition can be carried out in ambient and at low-annealing temperature. This method therefore opens up vast possibilities for deftly and straightforwardly printing complex devices, presenting many competitive advantages compared to other reported wet routes.

In conclusion, we have developed a cost-effective spray deposition methodology to fabricate high performance patterned OFETs via a surface energy difference-induced SAM even in a large scale. Depending on SAM patterns, the conjugated small molecule and polymer can be selectively spray-deposited on specific areas with oriented molecular packing. The proof-of-concept OFETs were found to operate at a charge carrier mobility almost one order of magnitude or several times higher than that deposited by conventional thin film without patterning. Organic semiconductor grown on the 4 inch substrate enables the large area OFETs to reveal excellent performance with high reliability and high yield. The self-organized assembly strategy combined with spray deposition described here is an easily scalable approach that tests the feasibility of patterned OFETs and is potential for the realization of large scale production of patterned organic electronic devices.

Experimental Section

Materials: All materials were used as received by the following suppliers. Sigma-Aldrich: anhydrous DCB. Gelest, Inc. (USA): all silanes including PETS, ODTS, OTS, MTMS, MPTMS, and CPTS. Poly(selenophene-alt-3,6-dithophene-2-yl-2,5-*bis*-(2-hexyldecyl)-2,5-dihydro-pyrrolo[3,4-c]pyrrole-1,4-dione) (PSeDPP; M_w ~ 96590 g mol^{-1}, polydispersity (PDI): 2.12) were synthesized according to the literature using Stille coupling reaction.

Characterization: The morphologies were characterized by optical microscope (Olympus BX51). The contact angle was measured using a high-resolution drop-shape analysis system (DSA 10-MK2, KRUESS, Germany) under laboratory conditions. GIXRD was performed on the beamline BL23A in the National Synchrotron Radiation Research Center (NSRRC), Taiwan.

Device Fabrication and Measurement: Heavily doped n-type Si wafer with 300 nm SiO_2 layer was diced, cleaned thoroughly with deionized water, acetone, and isopropyl alcohol for 10 min each in an ultrasonic bath, dried under nitrogen, and used immediately. The whole substrates were pretreated with ODTS and then selectively exposed to UV/ozone through a shadow mask for the removal of ODTS as well as definition of organic semiconductor layer. The defined area was modified with another silane SAM (with higher surface energy) listed above where it can serve as the wettable SAM to form the patterned area that the alkyl chains in ODTS were etched. A commercially available spray gun (Lumina GP-1 or AS-8, Japan) assembly was utilized for atomization of the coating solution (4 or 5 mg mL^{-1} of organic semiconductors in DCB) and deposition of the confined pattern of active layer. Spray parameters are summarized as follows: (1) pressurized N_2 gas: 25–40 psi; (2) solution feeding rate: 100–150 μL min^{-1}; (3) nozzle-to-sample distance: 10–15 cm; (4) spray time: 30–60 s; and (5) room temperature spray. The thickness of organic semiconductors is ~100 nm determined by surface profilometer. Following that, source and drain electrodes were defined on top of semiconducting layer by evaporating a 100 nm thick gold film at 0.5 Å s^{-1} through a shadow mask. All OFETs electrical characteristics were measured under N_2-atmosphere using a Keithley 4200-SCS semiconductor parameter analyzer.

Supporting Information

Supporting Information is available from the Wiley Online Library or from the author.

Acknowledgements

This work was supported by the Ministry of Science and Technology of Taiwan. The helpful discussion and instrumental support from Prof. Wen-Chang Chen and Dr. Hsuan-Chun Chang of National Taiwan University are highly appreciated.

Received: November 6, 2015
Revised: February 21, 2016
Published online: March 29, 2016

[1] A. Facchetti, *Mater. Today* **2007**, *10*, 28.
[2] C. Wang, H. Dong, W. Hu, Y. Liu, D. Zhu, *Chem. Rev.* **2012**, *112*, 2208.
[3] H. Dong, X. Fu, J. Liu, Z. Wang, W. Hu, *Adv. Mater.* **2013**, *25*, 6158.
[4] H. Sirringhaus, *Adv. Mater.* **2014**, *26*, 1319.
[5] J. Mei, Y. Diao, A. L. Appleton, L. Fang, Z. Bao, *J. Am. Chem. Soc.* **2013**, *135*, 6724.
[6] A. Facchetti, *Chem. Mater.* **2011**, *23*, 733.
[7] A. A. Virkar, S. Mannsfeld, Z. Bao, N. Stingelin, *Adv. Mater.* **2010**, *22*, 3857.
[8] Y. Diao, L. Shaw, Z. Bao, S. C. B. Mannsfeld, *Energy Environ. Sci.* **2014**, *7*, 2145.
[9] J. A. Lim, H. S. Lee, W. H. Lee, K. Cho, *Adv. Funct. Mater.* **2009**, *19*, 1515.
[10] C. K. Chan, L. J. Richter, B. Dinardo, C. Jaye, B. R. Conrad, H. W. Ro, D. S. Germack, D. A. Fischer, D. M. DeLongchamp, D. J. Gundlach, *Appl. Phys. Lett.* **2010**, *96*, 133304.
[11] A. Abdellah, B. Fabel, P. Lugli, G. Scarpa, *Org. Electron.* **2010**, *11*, 1031.
[12] L.-M. Chen, Z. Hong, W. L. Kwan, C.-H. Lu, Y.-F. Lai, B. Lei, C.-P. Liu, Y. Yang, *ACS Nano* **2010**, *4*, 4744.
[13] M. Shao, S. Das, K. Xiao, J. Chen, J. K. Keum, I. N. Ivanov, G. Gu, W. Durant, D. Li, D. B. Geohegan, *J. Mater. Chem. C* **2013**, *1*, 4384.
[14] D. Khim, K.-J. Baeg, B.-K. Yu, S.-J. Kang, M. Kang, Z. Chen, A. Facchetti, D.-Y. Kim, Y.-Y. Noh, *J. Mater. Chem. C* **2013**, *1*, 1500.
[15] H.-W. Hsu, C.-L. Liu, *RSC Adv.* **2014**, *4*, 30145.
[16] M. M. Ling, Z. N. Bao, *Chem. Mater.* **2004**, *16*, 4824.
[17] S. Liu, W. M. Wang, A. L. Briseno, S. C. E. Mannsfeld, Z. Bao, *Adv. Mater.* **2009**, *21*, 1217.
[18] A. C. Arias, J. D. MacKenzie, I. McCulloch, J. Rivnay, A. Salleo, *Chem. Rev.* **2010**, *110*, 3.
[19] J. Sun, B. Zhang, H. E. Katz, *Adv. Funct. Mater.* **2011**, *21*, 29.
[20] Y. Wen, Y. Liu, Y. Guo, G. Yu, W. Hu, *Chem. Rev.* **2011**, *111*, 3358.
[21] T. Minari, C. Liu, M. Kano, K. Tsukagoshi, *Adv. Mater.* **2012**, *24*, 299.
[22] B. Kang, W. H. Lee, K. Cho, *ACS Appl. Mater. Interfaces* **2013**, *5*, 2302.
[23] K.-J. Baeg, M. Caironi, Y.-Y. Noh, *Adv. Mater.* **2013**, *25*, 4210.
[24] Y. Li, H. Sun, Y. Shi, K. Tsukagoshi, *Sci. Technol. Adv. Mater.* **2014**, *15*, 024203.
[25] M. Ando, M. Kawasaki, S. Imazeki, H. Sasaki, T. Kamata, *Appl. Phys. Lett.* **2004**, *85*, 1849.
[26] A. L. Briseno, J. Aizenberg, Y. J. Han, R. A. Penkala, H. Moon, A. J. Lovinger, C. Kloc, Z. A. Bao, *J. Am. Chem. Soc.* **2005**, *127*, 12164.
[27] S. Liu, W. M. Wang, S. C. B. Mannsfeld, J. Locklin, P. Erk, M. Gomez, F. Richter, Z. Bao, *Langmuir* **2007**, *23*, 7428.

 © 2016 WILEY-VCH Verlag GmbH & Co. KGaA, Weinheim

ADVANCED MATERIALS INTERFACES
www.advmatinterfaces.de

[28] A. Salleo, A. C. Arias, *Adv. Mater.* **2007**, *19*, 3540.
[29] T. Minari, M. Kano, T. Miyadera, S.-D. Wang, Y. Aoyagi, M. Seto, T. Nemoto, S. Isoda, K. Tsukagoshi, *Appl. Phys. Lett.* **2008**, *92*, 173301.
[30] T. Minari, M. Kano, T. Miyadera, S.-D. Wang, Y. Aoyagi, K. Tsukagoshi, *Appl. Phys. Lett.* **2009**, *94*, 093307.
[31] H. S. Lee, D. Kwak, W. H. Lee, J. H. Cho, K. Cho, *J. Phys. Chem. C* **2010**, *114*, 2329.
[32] H. Minemawari, T. Yamada, H. Matsui, J. Tsutsumi, S. Haas, R. Chiba, R. Kumai, T. Hasegawa, *Nature* **2011**, *475*, 364.
[33] D. Choi, B. Ahn, S. H. Kim, K. Hong, M. Ree, C. E. Park, *ACS Appl. Mater. Interfaces* **2012**, *4*, 117.
[34] Y.-H. Kim, B. Yoo, J. E. Anthony, S. K. Park, *Adv. Mater.* **2012**, *24*, 497.
[35] G. Giri, S. Park, M. Vosgueritchian, M. M. Shulaker, Z. Bao, *Adv. Mater.* **2014**, *26*, 487.
[36] A. Pierre, M. Sadeghi, M. M. Payne, A. Facchetti, J. E. Anthony, A. C. Arias, *Adv. Mater.* **2014**, *26*, 5722.
[37] S. A. DiBenedetto, A. Facchetti, M. A. Ratner, T. J. Marks, *Adv. Mater.* **2009**, *21*, 1407.
[38] L. Miozzo, A. Yassar, G. Horowitz, *J. Mater. Chem.* **2010**, *20*, 2513.
[39] H. Ma, O. Acton, D. O. Hutchins, N. Cernetic, A. K. Y. Jen, *Phys. Chem. Chem. Phys.* **2012**, *14*, 14110.
[40] N. Saito, K. Hayashi, H. Sugimura, O. Takai, N. Nakagiri, *Chem. Phys. Lett.* **2001**, *349*, 172.
[41] H. Sugimura, K. Ushiyama, A. Hozumi, O. Takai, *Langmuir* **2000**, *16*, 885.
[42] G. Giri, E. Verploegen, S. C. B. Mannsfeld, S. Atahan-Evrenk, D. H. Kim, S. Y. Lee, H. A. Becerril, A. Aspuru-Guzik, M. F. Toney, Z. Bao, *Nature* **2011**, *480*, 504.
[43] Y. Diao, B. C. K. Tee, G. Giri, J. Xu, D. H. Kim, H. A. Becerril, R. M. Stoltenberg, T. H. Lee, G. Xue, S. C. B. Mannsfeld, Z. Bao, *Nat. Mater.* **2013**, *12*, 665.
[44] Y. Yuan, G. Giri, A. L. Ayzner, A. P. Zoombelt, S. C. B. Mannsfeld, J. Chen, D. Nordlund, M. F. Toney, J. Huang, Z. Bao, *Nat. Commun.* **2014**, *5*, 3005.
[45] H.-W. Lin, W.-Y. Lee, W.-C. Chen, *J. Mater. Chem.* **2012**, *22*, 2120.

© 2016 WILEY-VCH Verlag GmbH & Co. KGaA, Weinheim